High-Order Representation of Poincaré Maps

Johannes Grote, Martin Berz, and Kyoko Makino

Department of Physics and Astronomy, Michigan State University, East Lansing, MI, USA. {grotejoh,berz,makino}@msu.edu

Summary. A method to obtain polynomial approximations of Poincaré maps directly from a polynomial approximation of the flow or dynamical system for certain types of flows and Poincaré sections is presented. Examples for the method and its computational implementation are given.

Key words: Differential algebra, Poincaré map, dynamical systems.

1 Introduction

Poincaré maps are a standard tool in general dynamical systems theory to study qualitative properties of a dynamical system, e.g. the flow generated by an ordinary differential equation, most prominently the asymptotic stability of periodic or almost periodic orbits. A Poincaré map essentially describes how points on a plane S (the Poincaré section) which is transversed by such an orbit $\mathcal{O}$ (the reference orbit) and which are sufficiently close to $\mathcal{O}$ get mapped back onto S by the flow. The two key benefits in this approach are that long-term behavior of the the flow close to $\mathcal{O}$ can be analyzed through the derivative of the Poincaré map at the intersection point of S and $\mathcal{O}$, which is available after just one revolution of $\mathcal{O}$, and that the dimensionality of the problem has been reduced by one, since the Poincaré map is defined on S and neglects the "trivial" direction of the flow perpendicular to the surface.

In the numerical treatment of these problems one is faced with the question of which numerical representations of a flow are particularly favorable in the sense that they easily allow the computation of corresponding Poincaré maps for a given reference orbit and Poincaré section. In this paper we will show that high-order polynomial approximations of the flow, which have been obtained either by automatic differentiation of an ODE solver with respect to initial conditions or using differential algebraic (DA) tools as in [37,43], allow a direct deduction of polynomial approximations of Poincaré maps of a certain type. We focus on the case where the flow under consideration has been generated

by an ODE. The proposed algorithm is a part of an extended method for the computation of rigorous interval enclosures of the polynomial approximation of the Poincaré map discussed here.

2 Overview of DA Tools

The DA tools necessary to appreciate the method are described in detail in [37]. However, we wish to review briefly the two most important applications of DA-methods used for the problem discussed here: the DA-integration method employed to obtain high-order polynomial approximations $\varphi(x_0, t)$ of the flow and the functional inversion tools necessary in later steps of the algorithm.

2.1 DA-Integration of ODEs

First we tackle the problem of obtaining a polynomial approximation of the dependence on initial conditions of the solution of the initial value problem

$$\dot{x}(t) = f(x(t), t), \quad x(0) = X_0 + x_0 \ , \tag{1}$$

where $f : \mathbb{R}^\nu \supset U^{\text{open}} \longrightarrow \mathbb{R}^\nu$ is given as a composition of intrinsic functions which have been defined in DA-arithmetic. This also entails that f exhibits sufficient smoothness to guarantee existence and uniqueness of solutions for all initial conditions. The vector $X_0 \in \mathbb{R}^\nu$ is constant, and the midpoint of the domain box $D = [-d_1, d_1] \times \ldots \times [-d_\nu, d_\nu]$ for the small relative initial conditions $x_0 \in D$. Typical box widths d_i are of the order 10^{-2} to 10^{-8}. The polynomial approximation $\varphi(x_0, t)$ of the flow of (1) we desire is an expansion in terms of the independent time coordinate t and the initial conditions x_0 relative to X_0. The representation of this approximation is a DA-vector storing the expansion coefficients up to a prespecified order n in a structured fashion.

The standard procedure of a Picard iteration yields a polynomial approximation of the solution of (1) after repeated application of a Picard operator on the initial conditions. This iteration in general increases the order of the expansion by at least one in every step. Since a DA-vector can store coefficients up to order n, we expect that the iteration converges after finitely many steps in the DA case.

Accordingly, the Picard operator in the DA-computation is defined by

$$\mathcal{C}(\cdot) := (X_0 + x_0) + \partial_{\nu+1}^{-1} f(\cdot) \ ,$$

where f is computed in DA-arithmetic, and $\partial_{\nu+1}^{-1}$is the *antiderivation operator*, essentially the integration with respect to the ν+1st variable t. With a suitable definition of a contraction in the DA case, $\mathcal{C}$ is a contracting operator, and fixed-point theorems exist which guarantee that repeated applications of $\mathcal{C}$ on the initial condition DA-vector representation $x(0) = X_0 + x_0$ converge to the DA-vector solution $\varphi(x_0, t)$ of (1) in finitely many steps. After this iteration has converged, the time step is substituted for the time variable which yields the final solutions only in terms of the initial conditions x_0.

2.2 Functional Inversion Using DA-Arithmetic

Next we review the functional inversion method used to obtain the inverse $\mathcal{M}^{-1}$ of a function $\mathcal{M}$, or rather a DA-vector which stores the coefficients of $\mathcal{M}^{-1}$ up to the desired order. Assume we are given a smooth map $\mathcal{M} : \mathbb{R}^\nu \longrightarrow \mathbb{R}^\nu$ s.t. $\mathcal{M}(0) = 0$, and its linearization M is invertible at the origin. This assures the existence of a smooth inverse $\mathcal{M}^{-1}$ in a neighborhood of the origin. If we write $\mathcal{M} = M + \mathcal{N}$, where $\mathcal{N}$ is the nonlinear part, and insert this into the fundamental condition $\mathcal{M} \circ \mathcal{M}^{-1} = \mathcal{I}$, we obtain the relation

$$\mathcal{M}^{-1} = M^{-1} \circ (\mathcal{I} - \mathcal{N} \circ \mathcal{M}^{-1})$$

and see that the desired inverse $\mathcal{M}^{-1}$ is a fixed point of the operator $\mathcal{C}(\cdot) := M^{-1} \circ (\mathcal{I} - \mathcal{N} \circ \cdot)$. Since $\mathcal{C}$ is a contraction, the existence of the fixed point $\mathcal{M}^{-1}$ of $\mathcal{C}$ is verified, and $\mathcal{M}^{-1}$ can be obtained through repeated iteration of $\mathcal{C}$, beginning with the identity $\mathcal{I}$. Also in this case the iteration converges to $\mathcal{M}^{-1}$ in finitely many steps, which is intuitively clear: If at one iteration step $\mathcal{M}^{-1}$ is determined up to order m, then $\mathcal{C}(\mathcal{M}^{-1})$ is determined at least up to order $m + 1$, since $\mathcal{N}$ is purely nonlinear.

3 Description of the Method

3.1 Preliminary Remarks

We begin our discussion with the assumption that (1) exhibits a periodic solution $\varphi(X_0, t)$ which starts on a suitable Poincaré section and returns after a period T, which has been determined, e.g. by a high-order Runge-Kutta integration. As described in the previous section, there exist DA-arithmetic integration methods which allow us to transport the domain box $X_0 + D$, where $D = [-d_1, d_1] \times ... \times [-d_\nu, d_\nu]$, through one cycle of the period. In the last time step we keep the full expansion of the final solution $\varphi(x_0, t)$ in terms of the variables x_0 and the time t. The problem of constructing the Poincaré map has thus been reduced to the construction of a map which projects the set $\{\varphi(x_0, T) : x_0 \in D\}$ to the surface S.

We want to consider as large a class of surfaces as possible as Poincaré sections. A suitable assumption is that the Poincaré section $S \subset \mathbb{R}^\nu$ is given in terms of a function $\sigma : \mathbb{R}^\nu \longrightarrow \mathbb{R}$ as $S := \{x \in \mathbb{R}^\nu : \sigma(x) = 0\}$. Since the function σ also needs to be expressed in terms of elementary functions available in the computer environment for DA arithmetic, it is necessarily smooth, and hence so is the surface S. This contains most surfaces of practical interest, in particular the most common case where S is an affine plane $S := \{x \in \mathbb{R}^\nu : x_1 = c\}$ for some $c \in \mathbb{R}$; then $\sigma(x) = x_1 - c$.

3.2 Construction of the Crossing Time

The goal of the next step is to derive an expression for the crossing time $t_c(x_0)$ at which the trajectory starting at the initial condition $x_0 \in D$ crosses the

surface S. From an analytic standpoint the existence of such a time $t_c(x_0)$ is only guaranteed locally at X_0, but since usually D is small and σ and the vector field f are regular, the crossing time can often be defined for all $x_0 \in D$. Once we have obtained a DA-vector representing $t_c(x_0)$, then $\mathcal{P}(x_0)$ can be found easily by inserting the crossing time into the flow

$$\mathcal{P}(x_0) := \varphi(x_0, t_c(x_0)) \,, \tag{2}$$

where the right hand side is evaluated in DA-arithmetic. We proceed by constructing an artificial function $\psi(x_0, t)$ by

$$\begin{aligned} \psi_k(x_0, t) &:= x_k \,\forall\, k \in \{1, ..., \nu\} \\ \psi_{\nu+1}(x_0, t) &:= \sigma(\varphi(x_0, t)) \,. \end{aligned}$$

The value $t_c(x_0)$, depending on the variables x_0, is determined by the condition

$$\sigma(\varphi(x_0, t_c(x_0))) = 0 \,, \tag{3}$$

and ψ contains both the constraint (3) and the independent variables x_0. Because of (3), $t_c(x_0)$ satisfies

$$\psi(x_0, t_c(x_0)) = (x_0, 0) \,.$$

If ψ is invertible at $(x_0, t_c(x_0))$ we can evaluate

$$\psi^{-1}(x_0, 0) = \psi^{-1}(\psi(x_0, t_c(x_0))) = (x_0, t_c(x_0))^T$$

and immediately extract the DA-vector representation of $t_c(x_0)$ in terms of x_0 in the last component. However, here the invertibility of ψ at the point $(x_0, t_c(x_0))$ is guaranteed by the transversality of the flow at S. This leads to the definition of

$$t_c(x_0) := \psi_{\nu+1}^{-1}(x_0, 0) \,,$$

which allows us to obtain the final Poincaré map by construction (2).

3.3 Summary of the Algorithm

To conclude the presentation of the method, we summarize the algorithm:

1. Determine the period T approximately for the periodic orbit.
2. Choose a suitable Poincaré section S.
3. Obtain a DA-vector representation of the solution $\varphi(x_0, t)$ for one period T. Preserve the full expansion in x_0 and t in the last step.
4. Set up and invert the auxiliary function ψ using DA functional inversion to obtain a DA-vector representation of ψ^{-1}.
5. Resolve $t_c(x_0) := \psi^{-1}(x_0, 0)$.
6. Obtain $\mathcal{P}(x_0) := \varphi(x_0, t_c(x_0))$.

4 Examples

The method described above has been implemented in the COSY Infinity [42] programming language, which supports the DA-vector data type and its operations. The code lists for the example calculations are available upon request from the authors. The COSY output lists the Taylor expansion coefficients of $t_c(x_0)$ and $\mathcal{P}(x_0)$ sorted by order, with the last five columns showing the respective powers of the expansion variables $x_{0,1}$ through $x_{0,4}$ and t.

4.1 The Planar Kepler Problem

As a first example we study the planar Kepler problem,

$$\begin{aligned}\dot{x}_1 &= x_2 \\ \dot{x}_2 &= -\frac{x_1}{(x_1^2+x_3^2)^{3/2}} \\ \dot{x}_3 &= x_4 \\ \dot{x}_4 &= -\frac{x_3}{(x_1^2+x_3^2)^{3/2}}\ ,\end{aligned}$$

where we choose the initial conditions $x(0) = X_0 + x_0$. Here $X_0 = (0,-1,1,0)^T$ is the midpoint of the domain D for x_0 and the starting point for the reference orbit, and $D = [-10^{-4}, 10^{-4}]^4$. The reference orbit is periodic with a period $T = 2\pi$. The Poincaré section on which we project is $S := \{x \in \mathbb{R}^4 : x_1 = 0\}$.

The Kepler problem serves as a good test case, since not only the reference orbit, but all orbits originating in $X_0 + D$ are periodic. This means every trajectory crosses S at the same point where it originated after one revolution. Thus the ith component $\mathcal{P}_i(x_0)$ of the Poincaré map is the identity with respect to the expansion variable $x_{0,i}$. In the following, we show the results of the expansion coefficients of the crossing time $t_c(x_0)$ and the final components of $\mathcal{P}(x_0)$ after an 18th order computation. The result for the crossing time $t_c(x_0)$ is

```
  I  COEFFICIENT             ORDER EXPONENTS
  1  0.2731858587386304E-13   0   0 0  0 0  0
  2  0.3905776925772165E-03   1   1 0  0 0  0
  3  -.7362216057939549E-02   1   0 1  0 0  0
  4  0.7362216057939555E-02   1   0 0  1 0  0
  5  -.1651789475691988E-16   1   0 0  0 1  0
...
197  0.1730482119203762E-18   7   1 1  3 2  0
198  0.1875627603432954E-18   7   0 2  3 2  0
199  -.1075817722340857E-18   7   1 2  1 3  0
200  0.1018021833717433E-18   7   1 1  2 3  0
201  0.1149402904334884E-18   7   0 2  2 3  0,
```

where this is the expansion around the period $T = 2\pi$. We see that $t_c(x_0)$ has no constant part up to roughly machine precision and scales almost linearly with the variables $x_{0,1}$ to $x_{0,4}$, the second order terms are already significantly smaller.

Next we display the final result for the first component $\mathcal{P}_1(x_0)$. If the computed Poincaré map projects to the surface S, then its constant part must vanish. Indeed this is what we see up to leftover terms of negligible magnitude:

```
 I  COEFFICIENT             ORDER EXPONENTS
 1  -.2488159282559507E-19   2   0 2  0 0  0
 2  -.2482865326639168E-19   2   0 0  2 0  0.
```

Finally we give the result for $\mathcal{P}_2(x_0)$. In this case we restricted the Poincaré map $\mathcal{P}$ to S by setting $x_{0,1} = 0$. We see that $\mathcal{P}_2(x_0)$ preserves the first order identity in the $x_{0,2}$ variable up to a scaling factor of 10^{-4}, the domain half width. This rescaling supports validated computation.

```
 I  COEFFICIENT             ORDER EXPONENTS
 1  -.9999999999999988        0   0 0  0 0  0
 2  0.1000000000000023E-03    1   0 1  0 0  0
 3  -.1695071177393755E-17    1   0 0  1 0  0
 4  -.1850766989750646E-18    1   0 0  0 1  0
 5  0.3388131789017201E-19    2   0 2  0 0  0
...
34  0.2649298927416580E-19    7   0 2  5 0  0
35  -.2439099199128762E-19    7   0 5  1 1  0
36  0.5124187266775200E-19    7   0 4  2 1  0
37  0.5711061765338940E-19    7   0 3  3 1  0
38  0.2743591506567708E-19    7   0 2  4 1  0.
```

The results for $\mathcal{P}_3(x_0)$ and $\mathcal{P}_4(x_0)$ are similar to $\mathcal{P}_2(x_0)$.

4.2 A Muon Cooling Ring

In accelerator physics, a muon cooling ring is a simple representation of a device made up of solenoids, RF cavities, and hydrogen absorbers that is designed to 'cool' a muon particle beam, i.e. reduce the volume of phase space the beam occupies; for details see [5, 348, 421]. Its equations of motion are

$$\begin{aligned}
\dot{x}_1 &= x_3 \\
\dot{x}_2 &= x_4 \\
\dot{x}_3 &= x_4 - \frac{\alpha}{\sqrt{x_3^2 + x_4^2}}\, x_3 + \frac{\alpha}{\sqrt{x_1^2 + x_2^2}}\, x_2 \\
\dot{x}_4 &= -x_3 - \frac{\alpha}{\sqrt{x_3^2 + x_4^2}}\, x_4 - \frac{\alpha}{\sqrt{x_1^2 + x_2^2}}\, x_1 \,,
\end{aligned}$$

where $\alpha \in [0, 1]$ is the cooling parameter ($\alpha = 1$ being the fastest cooling), and we consider the initial values $x(0) = X_0 + x_0$ with $X_0 = (0, 1, 1, 0)^T$ and $D = [-10^{-4}, 10^{-4}]^4$. The centerpoint X_0 lies on a periodic orbit of the form $\varphi(0, t) =$

$(\cos(t), -\sin(t), -\sin(t), -\cos(t))$ with a period of $T = 2\pi$. However, no other orbit originating in the box $X_0 + (D \backslash \{0\})$ is periodic, but instead is slowly pulled towards the invariant solution $\varphi(0, t)$ with an asymptotic phase. This should be visible from the eigenvalues of the Poincaré map for the section $S := \{x \in \mathbb{R}^4 : x_1 = 0\}$. Again, we show the results for the crossing time $t_c(x_0)$ and the components of $\mathcal{P}(x_0)$ after an 18th order computation with a choice of $\alpha = 0.1$. For the crossing time $t_c(x_0)$ we obtain:

```
  I  COEFFICIENT             ORDER EXPONENTS
  1  0.2041481078081152E-13   0   0 0  0 0  0
  2  -.4881805626857354E-02   1   1 0  0 0  0
  3  0.1420453958184906E-03   1   0 1  0 0  0
  4  -.1420453958184956E-03   1   0 0  1 0  0
  5  0.1804749589528265E-02   1   0 0  0 1  0
...
 66  -.1728272108226884E-14   4   0 0  2 2  0
 67  -.1380573416990237E-15   4   1 0  0 3  0
 68  0.5285647002734696E-17   4   0 1  0 3  0
 69  0.4817909040734367E-14   4   0 0  1 3  0
 70  0.6371702406569035E-16   4   0 0  0 4  0.
```

This is the expansion around the period $T = 2\pi$. Inserting this into the flow $\varphi(x_0, t)$ and restricting $\varphi(x_0, t)$ to S yields that for $\mathcal{P}_1(x_0)$ all expansion coefficients are zero. For the component $\mathcal{P}_2(x_0)$ we get:

```
  I  COEFFICIENT             ORDER EXPONENTS
  1   1.000000000000000       0   0 0  0 0  0
  2  0.7300927710720673E-04   1   0 1  0 0  0
  3  0.2699072289279350E-04   1   0 0  1 0  0
  4  -.5747288684637408E-06   1   0 0  0 1  0
  5  -.1174080052084289E-08   2   0 2  0 0  0
...
 31  -.3092279715866550E-16   4   0 1  1 2  0
 32  0.5188804928611400E-16   4   0 0  2 2  0
 33  0.7267117814015809E-18   4   0 1  0 3  0
 34  -.3574718550317267E-17   4   0 0  1 3  0
 35  -.4144960345719535E-17   4   0 0  0 4  0;
```

for $\mathcal{P}_3(x_0)$:

```
  1   1.000000000000000       0   0 0  0 0  0
  2  -.3619742360532049E-19   1   0 1  0 0  0
  3  0.1000000000000003E-03   1   0 0  1 0  0
  4  -.1167493942379190E-08   2   0 2  0 0  0
  5  0.2334987884782753E-08   2   0 1  1 0  0
...
 30  -.9698631674909994E-17   4   0 1  1 2  0
 31  0.3092775905473012E-16   4   0 0  2 2  0
 32  0.7881782248585311E-18   4   0 1  0 3  0
 33  -.3750583012239952E-17   4   0 0  1 3  0
 34  -.4166566008579194E-17   4   0 0  0 4  0;
```

and for $\mathcal{P}_4(x_0)$:

```
  I  COEFFICIENT             ORDER EXPONENTS
  1  0.2775557561562886E-16   0   0 0  0 0  0
  2  0.5747288684637220E-06   1   0 1  0 0  0
  3  -.5747288684637250E-06   1   0 0  1 0  0
  4  0.7306674999405320E-04   1   0 0  0 1  0
  5  0.4038817974889429E-12   2   0 2  0 0  0
...
 31  0.3038943603851730E-18   4   0 1  1 2  0
 32  -.5017859446188993E-17   4   0 0  2 2  0
 33  0.2175112902784127E-18   4   0 1  0 3  0
 34  -.2064794267030274E-16   4   0 0  1 3  0
 35  0.1176604677592068E-17   4   0 0  0 4  0.
```

If we compute the eigenvalues of the linear part $P(x_{0,2}, x_{0,3}, x_{0,4})$ of $\mathcal{P}(x_0)$, when viewed as a function of $x_{0,2}$, $x_{0,3}$, and $x_{0,4}$, we get $\lambda_1 = 1$ and $\lambda_{2,3} \approx 0.73038 \pm i(0.00574)$. λ_1 is connected to the identity in the linear part of $\mathcal{P}_3(x_0)$ with respect to $x_{0,3}$, and the magnitude of less than 1 for λ_2 and λ_3 is a consequence of the cooling action in x_2- and x_4-directions, the desired effect of the muon cooler.

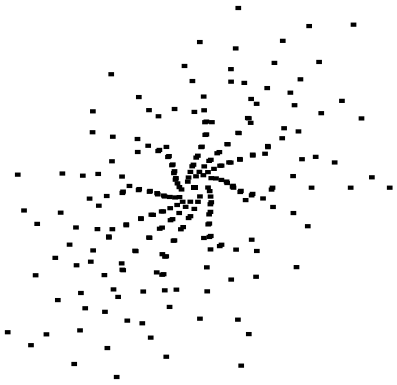

Fig. 1. Tracking of six particles for the first 50 turns in the muon cooling ring.

We use the Poincaré map for a detailed study of the dynamics by using it to iterate an ensemble of initial conditions through repeated orbits around the ring. This is an approach frequently followed in beam physics [37, 157], since it replaces time consuming integration of ODEs for one revolution by mere application of a polynomial. The results are shown in Fig. 1, showing the behavior in the transverse $x_{0,2}$-$x_{0,4}$-plane of an ensemble of six particles launched on the $x_{0,2}$-axis at the points $n \cdot 4$ cm for $n = 1, \ldots, 6$. The tracking picture is obtained after repeated application of the transverse components of the Poincaré map for 50 turns, and clearly exhibits the desired cooling effect near the attracting center.